Journal of Reproduction and Development, Vol. 63, No 3, 2017

—Original Article—

Ectopic expression of meiotic cohesin RAD21L promotes adjacency of homologous chromosomes in somatic cells

Mei RONG[1)], Sachi MIYAUCHI[1)] and Jibak LEE[1)]

[1)]*Laboratory of Developmental Biotechnology, Graduate School of Agricultural Science, Kobe University, Kobe 657-8501, Japan*

Abstract. Pairing, synapsis, and crossover recombination of homologous chromosomes (homologs) are prerequisite for the proper segregation of homologs during meiosis I. The meiosis-specific cohesin subunit, RAD21L, is essential for such meiotic chromosomal events, but it is unknown to what extent RAD21L by itself contributes to the process since various meiotic genes are also involved. To reveal the exclusive contribution of RAD21L to the specific regulation of homologs, we examined the effects of ectopic RAD21L expression on chromosome dynamics in somatic cells. We found that expression of GFP-fused RAD21L by plasmid transfection significantly shortened the distance between two FISH signals representing a pair of homologs for chromosome X or chromosome 11 in the nuclei compared to that in control (non-transfected) cells whereas expression of GFP-fused RAD21, a mitotic counterpart of RAD21L, showed no detectable effects. This indicates that RAD21L, when ectopically expressed in somatic cells, can promote homolog adjacency, which resembles the homolog pairing normally seen during meiosis. Furthermore, deletion of the N-terminal winged helix domain from RAD21L, prevented its association with another cohesin subunit, SMC3, and abolished the phenomenon of homolog adjacency upon ectopic expression. Our findings suggest that RAD21L-containing cohesin can promote homolog adjacency independently of other meiotic gene products, which might be central to the process of meiotic homolog paring.

Key words: Chromosome, Cohesin, Ectopic expression, Homolog paring, Meiosis

(**J. Reprod. Dev. 63:** 227–234, 2017)

Faithful segregation of chromosomes during mitosis and meiosis is the cornerstone of life. During mitosis, chromosomes are replicated and the resulting sister chromatids are segregated, generating two genetically identical daughter cells. Cohesion of sister chromatids is important for successful chromosome segregation in this process. On the other hand, meiosis is a highly specialized program of eukaryotic cell division that generates genetically diverse haploid gametes. This is accomplished by a single round of DNA replication followed by two successive rounds of chromosome segregation [1]. In meiosis I, homologous chromosomes (homologs) segregate, whereas in meiosis II, sister chromatids segregate. In order to ensure successful chromosome segregation during meiosis I, an association between homologs must be established by a series of coordinated events in prophase I, namely homolog paring, synapsis, and recombination [2, 3]. Homolog paring, the process in which homologs identify and create a physical association with their partners, occurs in the leptotene stage. Then, from the zygotene to pachytene stage, the association is strengthened and established along the chromosome axis in a process called synapsis, which is mediated by assembly of the synaptonemal complex, a meiosis-specific protein structure [2]. In parallel, recombination of homologs is initiated at the leptotene stage by SPO11-mediated DNA double strand breaks (DSBs), some of which are ultimately repaired as a crossover recombination at the pachytene stage [3]. It has been widely believed that DSBs also facilitate homolog pairing by providing a homology search based on DNA sequence. However, DSB-independent mechanisms of pairing have also been reported in various species including mammals [3–5]. Thus, how the homologs recognize and associate physically with one another is still a mystery. The inability to efficiently link homologs prior to their segregation leads to cell cycle arrest, apoptosis, or gamete aneuploidy, and chromosome missegregation during meiosis is a major cause of human miscarriage and developmental abnormalities [6]. Therefore, understanding the mechanisms establishing the link between homologs is important for both reproductive medicine and animal reproduction.

In mitosis, the cohesin complex facilitates sister chromatid cohesion and ensures chromosome segregation [7, 8]. In vertebrates, the mitotic cohesin complex consists of four subunits: two structural maintenance of chromosomes (SMC) subunits (SMC1α and SMC3), an α-kleisin subunit RAD21, and a heat repeat subunit, STAG1 or STAG2 [9, 10]. SMC1α and SMC3 interact with one another at a central hinge domain, and fold back on themselves through two long coiled-coil domains resulting in the juxtaposition of their head domains [11, 12]. The head domains of SMC1α and SMC3 bind to the C- and N-terminal winged helix domains of RAD21 respectively [11, 13, 14], thereby creating a tripartite ring-like cohesin complex in which sister chromatids can be entrapped [15]. Meiosis-specific cohesin subunits have been identified in various species of eukaryotes. Besides the canonical cohesin subunits, mammals have four meiosis-specific subunits: an SMC1 subunit (SMC1β) [16], two α-kleisins (RAD21L

Received: December 12, 2016
Accepted: February 6, 2017
Published online in J-STAGE: February 26, 2017

Correspondence: J Lee (e-mail: leej@tiger.kobe-u.ac.jp)

and REC8) [17–20], and a heat repeat subunit (STAG3) [21]. These meiotic subunits are involved in several aspects of meiotic chromosome dynamics including formation of the axial element (AE), synapsis and recombination of homologs, and cohesion of sister chromatids [22–28]. Since RAD21L is expressed exclusively in meiotic prophase I unlike other meiosis-specific cohesin subunits, it has been proposed that RAD21L is a special type of cohesin subunit dedicated to establishing the link between homologs [5, 19]. Recent studies using several lines of knockout (KO) mice [5] and high-resolution microscopy [29] have further clarified the differences in function and localization between RAD21L and REC8, and support this notion. However, the extent to which RAD21L by itself contributes to the process for establishing homolog association remains elusive.

To better understand the special role exclusively fulfilled by RAD21L in the process of homolog association, we ectopically expressed RAD21L fused with GFP (RAD21L-GFP) in somatic cells and examined its effects on chromosome dynamics by observing FISH signals representing a pair of homologs. Our study highlights a unique function of RAD21L in promoting homolog adjacency and sheds a new light on the molecular mechanism underlying the process of homolog pairing in meiosis.

Materials and Methods

Preparation of cDNA plasmid constructs

TrueORF clone vectors (pCMV6-ENTR vectors) expressing one of RAD21 (RAD21-DDK), REC8 (REC8-DDK), SMC3 (SMC3-DDK), or SMC1β (SMC1β-DDK) fused with a C-terminal Myc/DDK-tag were purchased from ORIGENE (Rockville, MD, USA). For the expression of GFP-fused RAD21 (RAD21-GFP) or REC8 (REC8-GFP), each of the ORFs was subcloned from the pCMV6-ENTR vectors into a precision destination vector (pCMV6-AC-mGFP, ORIGENE) at the *Sgf*I and *Mlu*I sites according to the manufacturer's instruction. For the expression of GFP-fused RAD21L (RAD21L-GFP), *Rad21l* cDNA [19] was amplified by PCR using the RAD21L forward primer (5′-TAGCGATCGCCATGTTCTACACTCATGT-3′; the *Sgf*I site is underlined) and RAD21L reverse primer (5′-GTACGCGTCATCTTATAGAACATTGGTCC-3′; the *Mlu*I site is underlined), and was then subcloned into the destination vector as described above.

The vector construct expressing the N-terminal 76-amino-acids-deleted RAD21L-GFP (RAD21LΔ76-GFP) was also prepared as follows. At first, a point mutation was inserted to create a new *Afl*II site using the QuikChange Site-Directed Mutagenesis Kit (Agilent Technologies, Santa Clara, CA, USA) with the mtRAD21L-fwd primer (5′-CACTCATGTGCTTAAGAGTAAACGGGGGC-3′; the *Afl*II site is underlined). The resultant vector construct had two *Afl*II sites spanning 228 base pairs just after the start codon of *Rad21l* cDNA. The regions flanked by the two *Afl*II sites were deleted from the clone vector by *Afl*II digestion followed by self-ligation. All constructs prepared in the present study, at least around the position of cDNA insertion or deletion, were verified by DNA sequencing.

Cell culture and transfection

The mouse embryonic fibroblast cell line NIH3T3 was obtained from Riken Cell Bank (RIKEN, Tsukuba, Japan). NIH3T3 cells were cultured in DMEM (Gibco, Life Technologies, Grand Island, NY, USA) containing 50 U/ml penicillin, 50 μg/ml streptomycin, and 10% heat-inactivated FBS (basic medium) at 37°C and 5% CO_2. The cells were seeded on 24-well plates at a density of 2.5×10^5 cells/ml. After 24 h of culture, cells were transfected for 6 h with 1 μg of plasmid DNA using the FuGENE 6 transfection reagent (Promega, Madison, WI, USA) in Opti-MEM (Gibco) according to the manufacturer's instructions. The transfected cells were then cultured in the basic medium for 24 h including 6 h of transfection.

In vitro assay for cohesin complex formation

For *in vitro* expression of SMC3-DDK, SMC1β-DDK, RAD21-GFP, RAD21L-GFP, RAD21LΔ76-GFP, and REC8-GFP, the respective vectors were added to TNT Quick Coupled transcription/translation Systems with methionine (Promega), according to the manufacturer's instruction. Then, for immunoprecipitation, the resultant products were incubated with the antibody against the DDK-tag for 1 h at 4°C with rotor agitation. After the addition of Protein A Sepharose (GE Healthcare, Uppsala, Sweden), the products were further incubated for 2 h. After 5 washes with TNE buffer (20 mM Tris-HCl, pH 7.4, 150 mM NaCl, 2 mM EDTA, 1% Nonidet P-40, 50 mM NaF, 1 mM Na_3VO_4, and 5 mM 2-mercaptoethanol), the immunoprecipitates were eluted with SDS sample buffer (62.5 mM Tris-HCl, pH 6.8, 1% SDS, 10% glycerol, 50 mM DTT, and 0.02% bromophenol blue) by boiling for 3 min and subsequently analyzed by SDS-PAGE followed by immunoblotting. Proteins from *in vitro* transcription/translation or from the immunoprecipitates were separated on 10% SDS polyacrylamide gels and transferred onto PVDF membranes (Thermo scientific, Billerica, MA, USA). Membranes were probed with anti-DDK (TA50011, ORIGENE), anti-RAD21, anti-RAD21L, or anti-REC8 [19] antibodies. Primary antibodies were detected by incubation with HRP-conjugated anti-rabbit IgG (GE Healthcare) or anti-mouse IgG (Dako, Glostrup, Denmark) antibodies and visualized using the ECL Prime Western Blotting Detection Reagent (GE Healthcare).

Fluorescence in situ hybridization (FISH) assay

After transfection, NIH3T3 cells were collected by centrifugation, treated with 0.56% KCl hypotonic solution for 20 min, and fixed by gradually adding fixative solution (methanol:acetic acid = 3:1). Then, the cells in the fixative solution were placed on the slides. The samples on slides were washed with 2 × SSC/0.5% Igepal (Wako) for 15 min at 37°C and subjected to sequential dehydration through 70%, 80%, 90%, and 100% ethanol. Hybridization was conducted with a fluorescence-labeled point probe and sealed overnight with a cover glass at 37°C. The slides were washed sequentially in 0.4 × SSC/0.3% Igepal for 1 min at 72°C and 2 × SSC/0.1% Igepal for 2 min at room temperature. Then, the samples were subjected to sequential dehydration through 70%, 80%, 90%, and 100% ethanol. The Rab9b (XqF1) and TK (11qE1) mouse point probes (Kreatech Diagnostics, Amsterdam, Netherlands) were used to detect the *Rab9b* gene on the chromosome X and the *Tlk2* gene on chromosome 11, respectively.

The distance between two FISH signals was measured for each nucleus of both transfected and non-transfected cells using the MetaMorph imaging program (Molecular Device, Downingtown,

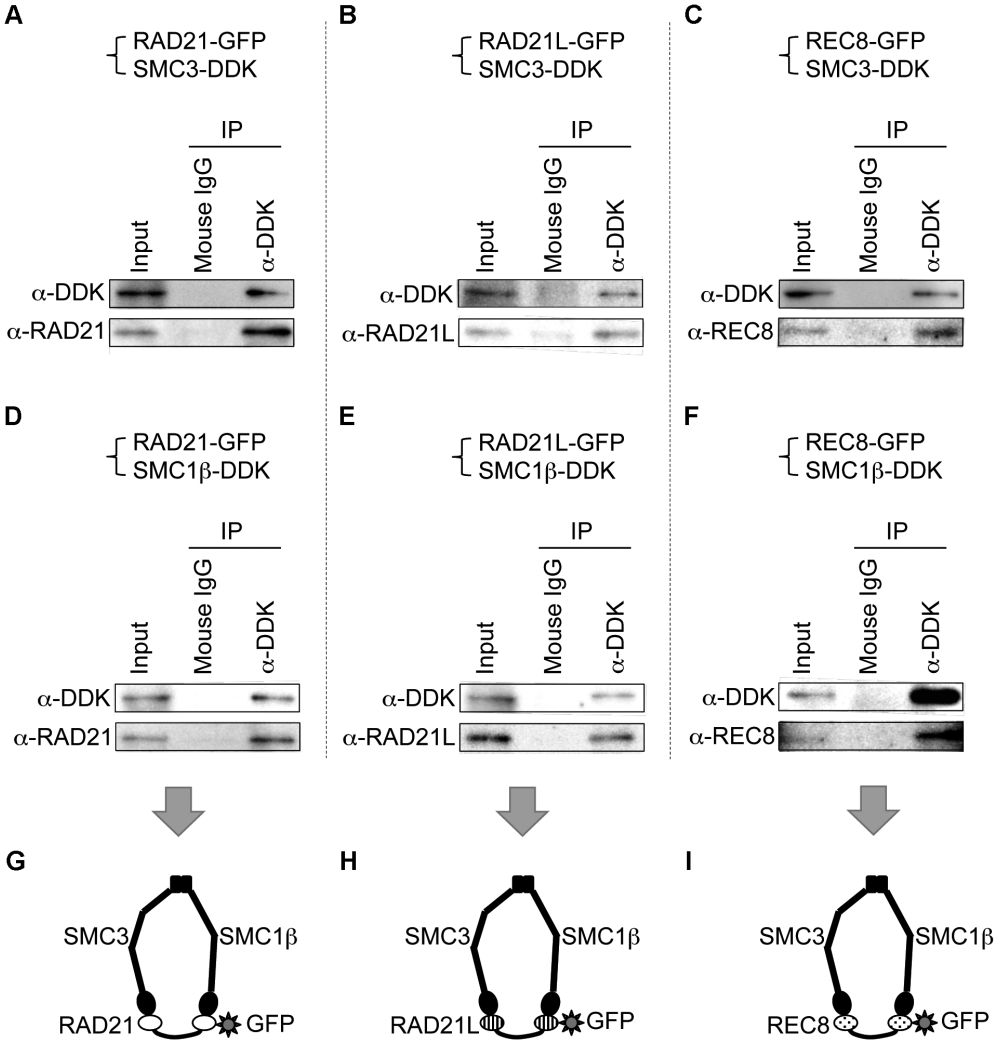

Fig. 1. *In vitro* binding assay of cohesin subunits. *In vitro* transcribed and translated cohesin subunits conjugated with DDK-tag or GFP-tag were mixed and co-immunoprecipitated with the anti-DDK antibody. The immunoprecipitates were subjected to western blotting using anti-DDK antibody and antibodies against the respective cohesin subunits indicated. The binding of RAD21-SMC3 (A), RAD21L-SMC3 (B), REC8-SMC3 (C), RAD21-SMC1β (D), RAD21L-SMC1β (E), and REC8-SMC1β (F) were tested. (G, H and I) A schematic illustration of the formation of cohesin complexes *in vitro*.

PA, USA). Significant differences between different samples were calculated using the Student's *t*-test.

Results

The three α-kleisins conjugated with GFP form a cohesin complex with SMC1β and SMC3 in vitro

Prior to examining the effects of the ectopic expression of meiotic cohesins in somatic cells, we checked whether cohesin subunits with the DDK-tag or GFP-tag are expressed from the plasmid constructs prepared in the present study and whether the three types of α-kleisins with C-terminal GFP can form cohesin complexes *in vitro*. The recombinant proteins expressed from constructs using the *in vitro* transcription/translation system were detected at the estimated electrophoretic mobility by SDS-PAGE followed by western blotting (data not shown). Then, we conducted co-immunoprecipitation assays by mixing the recombinant protein solutions. In the first set of experiments, we tested the binding of SMC3-DDK with RAD21-GFP (Fig. 1A), RAD21L-GFP (Fig. 1B), or REC8-GFP (Fig. 1C). All of α-kleisin-GFPs as well as SMC3-DDK were detected in the immunoprecipitates with the anti-DDK antibody, indicating that all the α-kleisin-GFPs associate with SMC3-DDK *in vitro*. Likewise, in the next set of experiments, we tested the binding of SMC1β-DDK with the α-kleisin-GFPs and found that α-kleisin-GFPs were co-immunoprecipitated with SMC1β-DDK (Fig. 1D–F). These results demonstrated that all three α-kleisin subunits can form a cohesin complex with SMC1β and SMC3 despite the presence of GFP-tag at their C-termini (Fig. 1G–I), as has been shown in

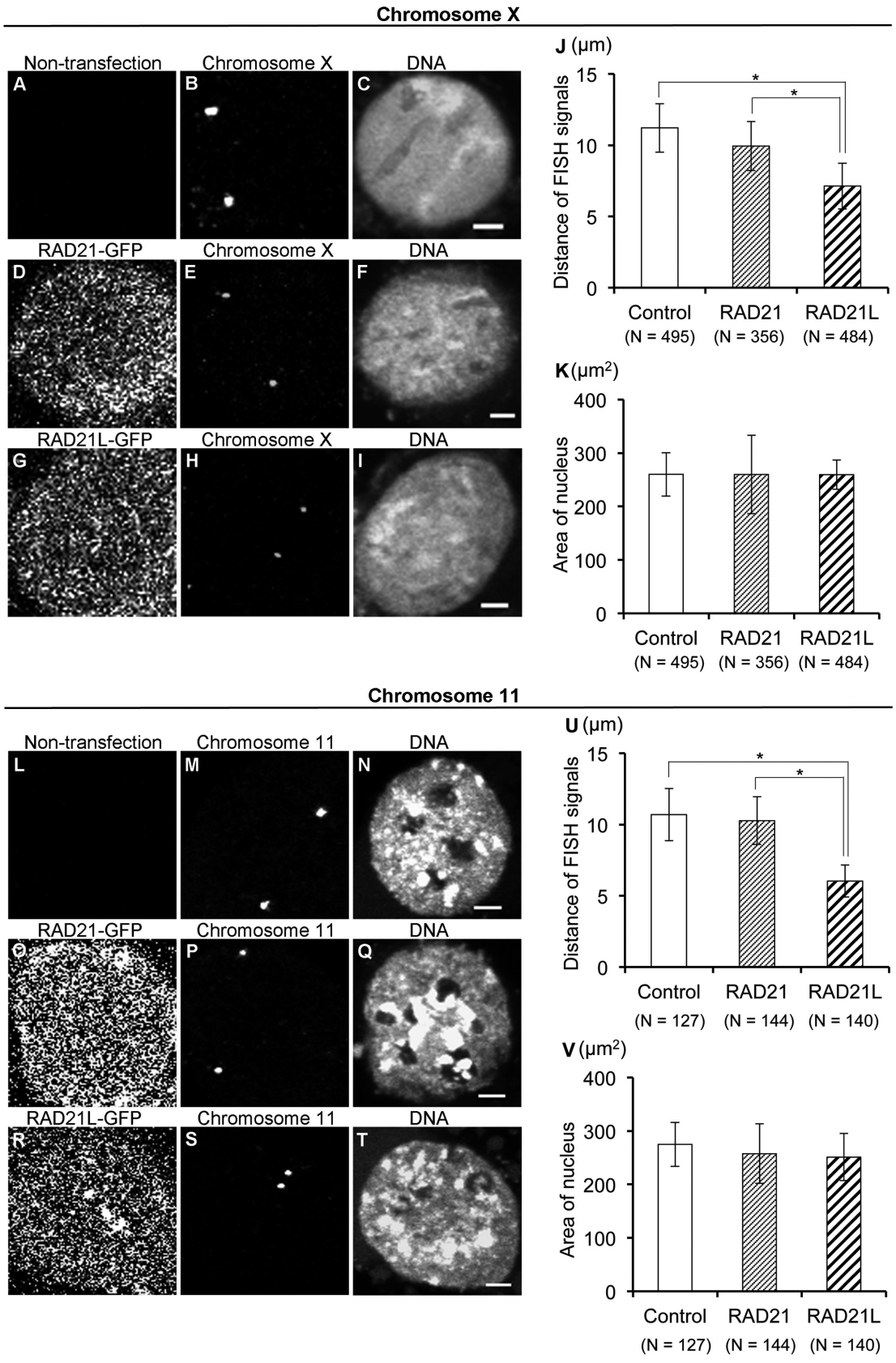
Chromosome X
Non-transfection
Chromosome X
DNA
A
B
C
RAD21-GFP
Chromosome X
DNA
D
E
F
RAD21L-GFP
Chromosome X
DNA
G
H
I
J (μm)
Distance of FISH signals
15
10
5
0
*
*
Control
RAD21
RAD21L
(N = 495)
(N = 356)
(N = 484)
K (μm²)
Area of nucleus
400
300
200
100
0
Control
RAD21
RAD21L
(N = 495)
(N = 356)
(N = 484)
Chromosome 11
Non-transfection
Chromosome 11
DNA
L
M
N
RAD21-GFP
Chromosome 11
DNA
O
P
Q
RAD21L-GFP
Chromosome 11
DNA
R
S
T
U (μm)
Distance of FISH signals
15
10
5
0
*
*
Control
RAD21
RAD21L
(N = 127)
(N = 144)
(N = 140)
V (μm²)
Area of nucleus
400
300
200
100
0
Control
RAD21
RAD21L
(N = 127)
(N = 144)
(N = 140)

Fig. 2.

previous reports using crude proteins from mouse testis extracts for co-immunoprecipitation assays [18, 19].

Ectopic expression of RAD21L brings homologs closer in somatic cells

Next, we tried to ectopically express the α-kleisin-GFPs in NIH3T3 cells by transfecting the constructs. The GFP signals of both RAD21-GFP and RAD21L-GFP were mostly detected in the nuclei and sometimes also in the cytoplasm of the transfected cells, although the transfection efficiency was very low (~2%) (Fig. 2D, G, O and R). Unlike these, REC8-GFP signals were detected mostly in the cytoplasm but hardly in the nuclei of the transfected cells (data not shown). Since REC8 is associated with SMC1β but not with SMC1α in testis extracts [17], we assumed that REC8-GFP might remain in the cytoplasm owing to inability to form a functional cohesin complex in somatic cells expressing only SMC1α. Therefore, we decided not to use REC8-GFP in the subsequent experiments.

To examine the effects of ectopic RAD21L expression in somatic cells, we conducted FISH assays using two kinds of point probes that detect a specific locus of chromosome X or chromosome 11. In the cells expressing RAD21-GFP, the distance between two FISH signals of the X chromosomes appeared similar to that in non-transfected (control) cells (Fig. 2B and E). On the other hand, in the cells expressing RAD21L-GFP, the distance between two FISH signals was apparently shorter than that in control or in RAD21-GFP-expressing cells (Fig. 2B, E and H). Thus, we measured and compared the distance between FISH signals across the experimental groups as well as the areas of the nuclei as internal controls. The distance between FISH signals in RAD21L-GFP-expressing cells (7.134 ± 1.609 μm) was significantly shorter than that in control cells (11.215 ± 1.706 μm) or that in RAD21-GFP-expressing cells (9.937 ± 1.719 μm) (Fig. 2J), whereas the areas of nuclei were similar in all the groups (Fig. 2K). Using the FISH probe for chromosome 11, we obtained essentially the same results; the distance between FISH signals in RAD21L-GFP-expressing cells was significantly shorter than that in control cells or that in RAD21-GFP-expressing cells (Control: 10.690 ± 1.822 μm; RAD21-GFP: 10.269 ± 1.679 μm; RAD21L-GFP: 6.032 ± 1.115 μm) (Fig. 2U). These results indicate that the ectopic expression of RAD21L brings homologs closer, at least in two pairs of homologs including both the sex and autosomal chromosomes, in the nuclei of somatic cells. In the present study, the phenomenon wherein homologs come closer upon ectopic expression of RAD21L was termed as homolog adjacency to distinguish it from the process of homolog association normally observed in meiosis, such as paring and synapsis.

Deletion of N-terminal winged helix domain of RAD21L abolished its abilities of forming a cohesin complex and promoting homolog adjacency

To confirm the effect of the ectopic expression of RAD21L, we prepared a construct expressing a mutant RAD21L-GFP having a 76-amino-acid deletion in the N-terminal winged helix domain (RAD21LΔ76-GFP), which is a conserved domain among the three types of α-kleisin [19]. Using this construct, we first conducted an *in vitro* binding assay for the cohesin complex, and found that RAD21LΔ76-GFP was co-immunoprecipitated with SMC1β-DDK (Fig. 3A) but not with SMC3-DDK (Fig. 3B), indicating that the N-terminal winged helix domain is essential for binding to SMC3, that is, for the assembly of a functional cohesin complex (Fig. 3C). We then conducted FISH assays in NIH3T3 cells and compared the results between RAD21L-GFP and RAD21LΔ76-GFP (Fig. 4A–I and L–T). The distance between two FISH signals in RAD21LΔ76-GFP-expressing cells was similar to that in control cells but was significantly greater than that in RAD21L-GFP-expressing cells regardless of the kind of probes used for FISH analyses (Fig. 4J and U), indicating that the distance shortening effect by ectopic expression of RAD21L is abolished by deletion of the N-terminal winged helix domain.

Altogether, these results suggest that RAD21L promotes the adjacency of homologs, probably by forming a cohesin complex when it is expressed in somatic cells.

Discussion

To ensure the accurate separation of homologs in meiosis I, an association between homologs must be established in prophase I. Several layers of mechanisms such as telomere-led nuclear movement, DSB-dependent recombination, synaptonemal complex assembly, and sister chromatid cohesion contribute to homolog association [3, 30]. Previous studies suggest that meiotic cohesins are central to the process of homolog association [5, 16, 24, 26, 31]. Among several meiotic cohesin subunits, cytological and genetic studies have suggested that RAD21L is a special type of cohesin subunit dedicated to the establishment of homolog association [5, 18, 19, 29]. However, the extent to which RAD21L by itself contributes to the process remains elusive because many meiotic genes are also involved. In the present study, we examined the effects of ectopically expressed RAD21L on chromosome dynamics in somatic cells, that is, under circumstances excluding the influence of other meiotic genes. We found that the distance between two FISH signals representing homologs was significantly shortened in RAD21L-GFP-expressing cells but not in RAD21-GFP-expressing cells compared to that in control cells (Fig. 2), indicating that ectopic expression of RAD21L is sufficient to promote homolog adjacency in somatic cells. Future studies should investigate whether ectopic expression of RAD21L promotes homolog adjacency in all pairs of homologs. We also found that deletion of the N-terminal winged helix domain of RAD21L, which made RAD21L unable to form a functional cohesin complex, abolished its ability to promote homolog adjacency (Fig. 4). Therefore, we assume that RAD21L probably forms a cohesin complex in somatic

Fig. 2. Meiosis-specific cohesin subunit RAD21L brings homologs closer in somatic cells. Non-transfected NIH3T3 cells (A–C and L–N) and NIH3T3 cells transfected with a RAD21-GFP construct (D–F and O–Q) or a RAD21L-GFP construct (G–I and R–T) were subjected to FISH analysis with a point probe for chromosome X or chromosome 11. DNA was counterstained with DAPI. Scale bars: 2 μm. The distances between two FISH signals of chromosome X (J) and chromosome 11 (U) are shown in the graph (* $P < 0.01$ by *t*-test). (K and V) The areas of the nuclei are shown in the graph. (Control) Non-transfected cells; (RAD21) RAD21-GFP-expressing cells; (RAD21L) RAD21L-GFP-expressing cells.

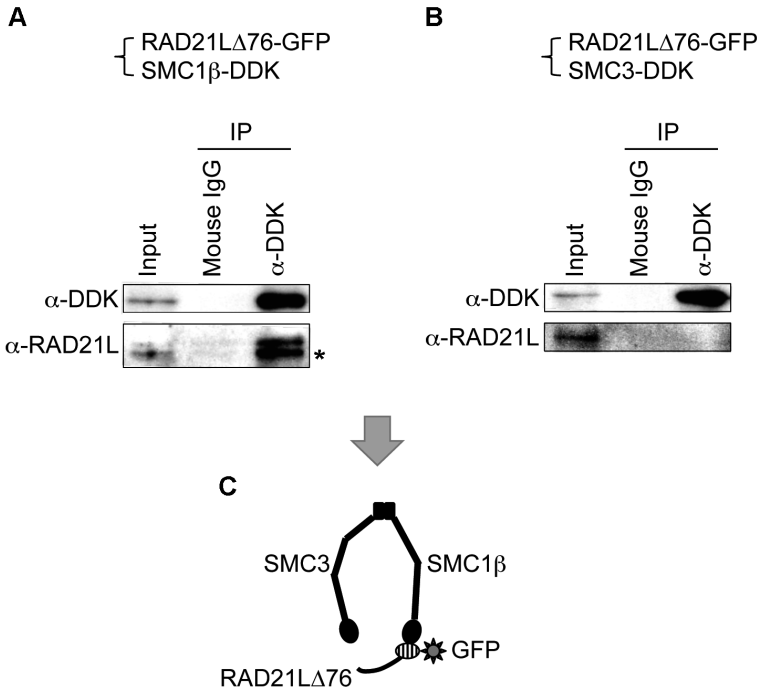

Fig. 3. *In vitro* binding assay of the RAD21L deletion mutant. *In vitro* transcribed and translated cohesin subunits conjugated with the DDK-tag or GFP-tag were mixed and co-immunoprecipitated with the anti-DDK antibody. The immunoprecipitates were subjected to western blotting using anti-DDK and anti-RAD21L antibodies. The binding of RAD21LΔ76-SMC1β (A) and RAD21LΔ76-SMC3 (B) were tested. The smaller-sized band indicated by the asterisk presumably represents a partially degraded form of RAD21LΔ76-GFP. (C) Schematic illustration of the formation of the cohesin complex *in vitro*.

cells, which is required for promoting homolog adjacency. However, we cannot exclude an alternative possibility that the deleted domain itself might be essential for RAD21L function. In either case, the present study elucidated a novel function for RAD21L.

The RAD21L-promoted homolog adjacency seems to resemble the chromosome dynamics normally seen in meiotic prophase I. It has been suggested that RAD21L is essential for several meiotic chromosome dynamics such as paring, synapsis, and recombination of homologs [26]. RAD21L also contributes to the formation of AEs, cooperatively with REC8, since AEs are absent in the double KO spermatocytes [27]. We assume that homolog adjacency might be equivalent to the initial stage of pairing at pre-leptotene or early leptotene because any special chromosome axes, such as cohesin cores or AEs, were not observed in somatic cells expressing RAD21L as judged by the GFP signals (Fig. 2G). In this context, a recent study using several lines of KO mice suggests that RAD21L, but not REC8, is required for the recognition and pairing of homologs that are independent of both telomere-led nuclear movement and DSB formation [18]. Our findings strongly support this view since Spo11-mediated DSB formation and telomere-led nuclear movement including “bouquet” arrangement are both absent in somatic cells, though the possibility that Spo11-independent DSBs, which are often observed in cultured somatic cells might facilitate the function of RAD21L, is still debatable. In meiocytes, RAD21L potentially makes several types of cohesin complexes by associating with other meiosis-specific cohesin subunits (SMC1β, STAG3) as well as ubiquitous cohesin subunits (SMC1α, STAG1/STAG2, SMC3). Thus, it is hard to identify which cohesin complex containing RAD21L is required for homolog pairing. Our study using somatic cells circumvents this issue and suggests that RAD21L can promote homolog adjacency by forming a cohesin complex that excludes other meiosis-specific cohesin subunits, that is a cohesin complex consisting of RAD21L, SMC1α, SMC3, and either STAG1 or STAG2, if it formed a complex. How RAD21L recognizes and links homologs remains an open question for future study.

In conclusion, we showed that ectopic expression of a single meiotic gene product, RAD21L, can promote homolog adjacency that resembles homolog pairing in meiosis. This finding not only advances our understanding of the mechanisms governing meiotic chromosome dynamics but also provides the first step to artificial haploidization of somatic cells for application to reproductive biotechnology.

Acknowledgments

We are grateful to the members of our laboratory for their valuable support and discussions. This work was supported in part by JSPS KAKENHI (Grant Numbers 26292169 to JL).

References

1. **Nasmyth K.** Segregating sister genomes: the molecular biology of chromosome separation. *Science* 2002; **297**: 559–565. [Medline] [CrossRef]
2. **Page SL, Hawley RS.** The genetics and molecular biology of the synaptonemal complex. *Annu Rev Cell Dev Biol* 2004; **20**: 525–558. [Medline] [CrossRef]

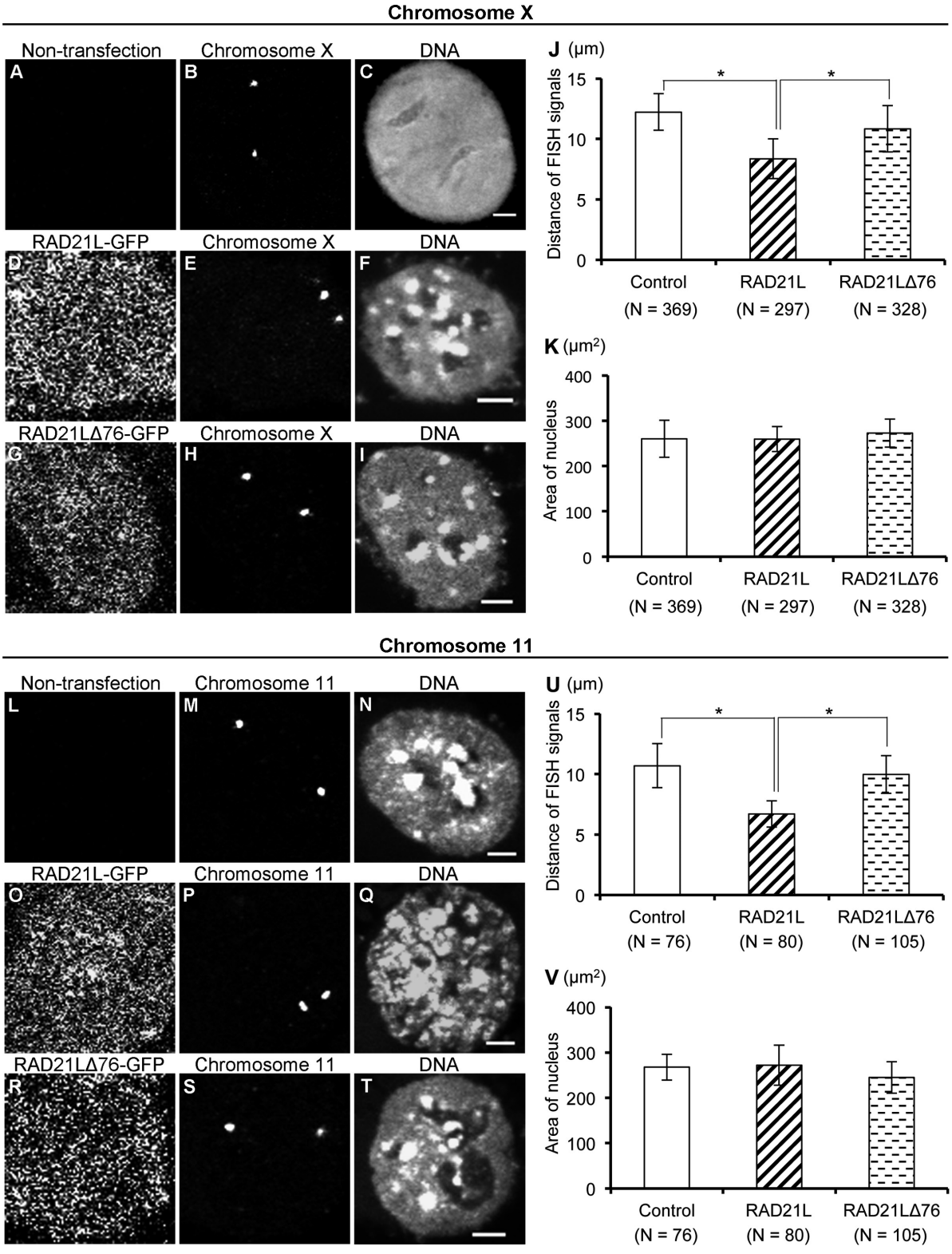

Fig. 4. Deletion of the N-terminal winged helix domain from RAD21L abolished its ability to promote homolog adjacency. Non-transfected NIH3T3 cells (A–C and L–N) and NIH3T3 cell transfected with the RAD21L-GFP construct (D–F and O–Q) or RAD21LΔ76-GFP construct (G–I and R–T) were subjected to FISH analysis with a point probe for chromosome X or chromosome 11. DNA was counterstained with DAPI. Scale bars: 2 μm. The distances between two FISH signals of chromosome X (J) and chromosome 11 (U) are shown in the graph (* $P < 0.01$ by *t*-test). (K and V) The areas of the nuclei are shown in the graph. (Control) Non-transfected cells; (RAD21L) RAD21L-GFP-expressing cells; (RAD21LΔ76) RAD21LΔ76-GFP-expressing cells.

3. **Zickler D, Kleckner N.** Recombination, pairing, and synapsis of homologs during meiosis. *Cold Spring Harb Perspect Biol* 2015; **7**: a016626. [Medline] [CrossRef]
4. **Boateng KA, Bellani MA, Gregoretti IV, Pratto F, Camerini-Otero RD.** Homologous pairing preceding SPO11-mediated double-strand breaks in mice. *Dev Cell* 2013; **24**: 196–205. [Medline] [CrossRef]
5. **Ishiguro K, Kim J, Shibuya H, Hernández-Hernández A, Suzuki A, Fukagawa T, Shioi G, Kiyonari H, Li XC, Schimenti J, Höög C, Watanabe Y.** Meiosis-specific cohesin mediates homolog recognition in mouse spermatocytes. *Genes Dev* 2014; **28**: 594–607. [Medline] [CrossRef]
6. **Nagaoka SI, Hassold TJ, Hunt PA.** Human aneuploidy: mechanisms and new insights into an age-old problem. *Nat Rev Genet* 2012; **13**: 493–504. [Medline] [CrossRef]
7. **Nasmyth K.** Disseminating the genome: joining, resolving, and separating sister chromatids during mitosis and meiosis. *Annu Rev Genet* 2001; **35**: 673–745. [Medline] [CrossRef]
8. **Hirano T.** The ABCs of SMC proteins: two-armed ATPases for chromosome condensation, cohesion, and repair. *Genes Dev* 2002; **16**: 399–414. [Medline] [CrossRef]
9. **Losada A, Hirano M, Hirano T.** Identification of Xenopus SMC protein complexes required for sister chromatid cohesion. *Genes Dev* 1998; **12**: 1986–1997. [Medline] [CrossRef]
10. **Sumara I, Vorlaufer E, Gieffers C, Peters BH, Peters JM.** Characterization of vertebrate cohesin complexes and their regulation in prophase. *J Cell Biol* 2000; **151**: 749–762. [Medline] [CrossRef]
11. **Haering CH, Löwe J, Hochwagen A, Nasmyth K.** Molecular architecture of SMC proteins and the yeast cohesin complex. *Mol Cell* 2002; **9**: 773–788. [Medline] [CrossRef]
12. **Anderson DE, Losada A, Erickson HP, Hirano T.** Condensin and cohesin display different arm conformations with characteristic hinge angles. *J Cell Biol* 2002; **156**: 419–424. [Medline] [CrossRef]
13. **Hirano M, Hirano T.** Hinge-mediated dimerization of SMC protein is essential for its dynamic interaction with DNA. *EMBO J* 2002; **21**: 5733–5744. [Medline] [CrossRef]
14. **Nasmyth K, Haering CH.** The structure and function of SMC and kleisin complexes. *Annu Rev Biochem* 2005; **74**: 595–648. [Medline] [CrossRef]
15. **Gruber S, Haering CH, Nasmyth K.** Chromosomal cohesin forms a ring. *Cell* 2003; **112**: 765–777. [Medline] [CrossRef]
16. **Revenkova E, Eijpe M, Heyting C, Hodges CA, Hunt PA, Liebe B, Scherthan H, Jessberger R.** Cohesin SMC1 beta is required for meiotic chromosome dynamics, sister chromatid cohesion and DNA recombination. *Nat Cell Biol* 2004; **6**: 555–562. [Medline] [CrossRef]
17. **Lee J, Iwai T, Yokota T, Yamashita M.** Temporally and spatially selective loss of Rec8 protein from meiotic chromosomes during mammalian meiosis. *J Cell Sci* 2003; **116**: 2781–2790. [Medline] [CrossRef]
18. **Ishiguro K, Kim J, Fujiyama-Nakamura S, Kato S, Watanabe Y.** A new meiosis-specific cohesin complex implicated in the cohesin code for homologous pairing. *EMBO Rep* 2011; **12**: 267–275. [Medline] [CrossRef]
19. **Lee J, Hirano T.** RAD21L, a novel cohesin subunit implicated in linking homologous chromosomes in mammalian meiosis. *J Cell Biol* 2011; **192**: 263–276. [Medline] [CrossRef]
20. **Eijpe M, Offenberg H, Jessberger R, Revenkova E, Heyting C.** Meiotic cohesin REC8 marks the axial elements of rat synaptonemal complexes before cohesins SMC1beta and SMC3. *J Cell Biol* 2003; **160**: 657–670. [Medline] [CrossRef]
21. **Prieto I, Suja JA, Pezzi N, Kremer L, Martínez-A C, Rufas JS, Barbero JL.** Mammalian STAG3 is a cohesin specific to sister chromatid arms in meiosis I. *Nat Cell Biol* 2001; **3**: 761–766. [Medline] [CrossRef]
22. **Klein F, Mahr P, Galova M, Buonomo SB, Michaelis C, Nairz K, Nasmyth K.** A central role for cohesins in sister chromatid cohesion, formation of axial elements, and recombination during yeast meiosis. *Cell* 1999; **98**: 91–103. [Medline] [CrossRef]
23. **Watanabe Y, Nurse P.** Cohesin Rec8 is required for reductional chromosome segregation at meiosis. *Nature* 1999; **400**: 461–464. [Medline] [CrossRef]
24. **Xu H, Beasley MD, Warren WD, van der Horst GT, McKay MJ.** Absence of mouse REC8 cohesin promotes synapsis of sister chromatids in meiosis. *Dev Cell* 2005; **8**: 949–961. [Medline] [CrossRef]
25. **Novak I, Wang H, Revenkova E, Jessberger R, Scherthan H, Höög C.** Cohesin Smc1beta determines meiotic chromatin axis loop organization. *J Cell Biol* 2008; **180**: 83–90. [Medline] [CrossRef]
26. **Herrán Y, Gutiérrez-Caballero C, Sánchez-Martín M, Hernández T, Viera A, Barbero JL, de Álava E, de Rooij DG, Suja JÁ, Llano E, Pendás AM.** The cohesin subunit RAD21L functions in meiotic synapsis and exhibits sexual dimorphism in fertility. *EMBO J* 2011; **30**: 3091–3105. [Medline] [CrossRef]
27. **Llano E, Herrán Y, García-Tuñón I, Gutiérrez-Caballero C, de Álava E, Barbero JL, Schimenti J, de Rooij DG, Sánchez-Martín M, Pendás AM.** Meiotic cohesin complexes are essential for the formation of the axial element in mice. *J Cell Biol* 2012; **197**: 877–885. [Medline] [CrossRef]
28. **Fukuda T, Fukuda N, Agostinho A, Hernández-Hernández A, Kouznetsova A, Höög C.** STAG3-mediated stabilization of REC8 cohesin complexes promotes chromosome synapsis during meiosis. *EMBO J* 2014; **33**: 1243–1255. [Medline]
29. **Rong M, Matsuda A, Hiraoka Y, Lee J.** Meiotic cohesin subunits RAD21L and REC8 are positioned at distinct regions between lateral elements and transverse filaments in the synaptonemal complex of mouse spermatocytes. *J Reprod Dev* 2016; **62**: 623–630. [Medline] [CrossRef]
30. **Hiraoka Y, Dernburg AF.** The SUN rises on meiotic chromosome dynamics. *Dev Cell* 2009; **17**: 598–605. [Medline] [CrossRef]
31. **Biswas U, Wetzker C, Lange J, Christodoulou EG, Seifert M, Beyer A, Jessberger R.** Meiotic cohesin SMC1β provides prophase I centromeric cohesion and is required for multiple synapsis-associated functions. *PLoS Genet* 2013; **9**: e1003985. [Medline] [CrossRef]